CTU Journal of Innovation and Sustainable Development
ISSN 2588-1418 | e-ISSN 2815-6412

DOI:10.22144/ctujoisd.2026.026

Removal of methyl violet from aqueous solution using chemically modified biochar derived from corncob

Nhut Minh Nguyen[1*], Thong Phuc Lam[2], Lan Nguyen Phuong Tran[3], and Dang Huynh Giao[2]

[1]*Materials Energy Lab, Faculty of Chemical Engineering, Can Tho University, Viet Nam*

[2]*Faculty of Chemical Engineering, Can Tho University, Viet Nam*

[3]*Faculty of Mechanical Engineering, Can Tho University, Viet Nam*

**Corresponding author (nmnhut@ctu.edu.vn)*

Article info.

Received 28 Apr 2025
Revised 15 May 2025
Accepted 26 Dec 2025

Keywords

Adsorption, biochar, chemical modification, corncob, methyl violet

ABSTRACT

Chemically modified corncob biochar was prepared to remove methyl violet, an organic dye, from simulated wastewater. Modern analytical methods, including SEM, FT-IR, BET/pore, etc., indicated that the porous biochar exhibited excellent characteristics, with a high specific surface area (989.14 m^2/g), a large pore volume (0.61 cm^3/g), and abundant functional groups on its surface. Consequently, it achieved high removal efficiency for methyl violet, with an adsorption capacity of 290.7 mg/g and a removal rate of 92.4% at high concentrations. The Pseudo-first-order and Temkin models can effectively simulate the kinetic and isotherm adsorption processes of BioPNa for MV, with $R^2 > 0.99$, indicating physicochemical composite processes as the adsorption mechanisms, including pore filling, electrostatic attractions, hydrogen bonds, and π-π interactions. The porous material also demonstrated high stability and reusability after five adsorption-desorption cycles. Therefore, it can be used as a low-cost, high-efficiency material for effectively removing methyl violet from wastewater.

1. INTRODUCTION

The social economy has grown rapidly, discharging large amounts of wastewater into surface waters and groundwater (Wang et al., 2021). Among harmful contaminants, dyes are widely used in industrial applications; however, a large amount of unused dye is released into the natural environment, resulting in serious pollution (Tran-Nguyen et al., 2025). Methyl violet (MV), a synthetic dye with a complex molecular structure, poses significant threats to both the environment and human health. Recently, biochar prepared from agricultural wastes has attracted the attention of many researchers for its effectiveness in removing various pollutants, owing to its eco-friendly nature, reusability, and cost-effectiveness (Yaashikaa et al., 2020). The removal of dibenzothiophene on activated carbon derived from coconut was determined in the presence of benzene and olefins. The removal rate of dibenzothiophene decreased with increasing hydrocarbon concentration in the presence of benzene in the mixture, whereas the olefin in the system could prevent its adsorption (Yu et al., 2008). An investigation of dye removal on microporous phenolic resin-based activated carbon fibers in a binary system showed that Congo red blocks the active adsorbent sites, preventing the adsorption of atrazine. It was also found that increasing the average pore size of a solid material promoted competition in the system (Pelekani & Snoeyink, 2001). The simultaneous adsorption of methylene blue and Rhodamine B was studied using

activated carbon prepared from orange peel. Both dyes have been reported to adversely affect mutual adsorption (Fernandez et al., 2014). Bustard et al (1998) found that high initial concentrations of dyes offered a strong force to overcome all mass transfer resistance between solid and aqueous phases (Bustard et al., 1998; Bustard et al., 1998; Bustard et al., 1998). Recent developments in biochar activation techniques have significantly increased adsorption capacity, making biochar a promising approach for wastewater treatment (Nguyen et al., 2024). Biochar can be physically or chemically modified to achieve the desired surface properties (Sajjadi et al., 2018; Sajjadi et al., 2019). Improving its properties can enhance the contaminant removal rate in aqueous solutions. It was reported that biochar from phenol-formaldehyde (PF) resin-treated wood, which was further modified with KOH, exhibited a remarkable porous structure and abundant functional groups on its surface, resulting in very high adsorption capacity for methylene blue (1112 mg/g) and congo red (> 3472 mg/g) (Zhang et al., 2024). Thus, it is promising for widespread use in environmental protection, particularly for removing organic pollutants from wastewater and the chemical industry. However, combining two chemically activated steps for biochar modification has rarely been reported in the current literature, resulting in a lack of understanding of the behavior and changes in biochar properties during the activation and adsorption processes (Nguyen et al., 2024; Sajjadi et al., 2019). Consequently, this may hinder large-scale applications.

In this study, NaOH- and H_3PO_4-modified corncob biochar was prepared to investigate the feasibility of methyl violet removal from aqueous solutions. The modified biochar was characterized to determine its intrinsic properties and the relationship between these properties and the MV adsorption efficacy. Various adsorption parameters, including contact time, mass dosage of biochar, and MV concentration, were analyzed to determine their effects on adsorption performance. Additionally, the stability and reusability of the porous material were evaluated through multiple adsorption cycles. The results of the adsorption kinetics and isotherm analyses can predict the adsorption behavior and suggest the mechanisms occurring in the adsorption process. Therefore, this study provides valuable insights into the effective treatment of organic contaminants using porous materials derived from agricultural waste.

2. MATERIALS AND METHODS

2.1. Materials and chemicals

Sodium hydroxide (NaOH, ≥ 96,0 % purity), methanol (99,5%), and hydrogen peroxide (H_2O_2, 30%) were bought from Xilong Chemicals, China; Phosphoric acid (H_3PO_4, 75,0-85,0 %) and methyl violet ($C_{24}H_{28}ClN_3$, ≥ 99,0% purity) were from DaoMao, China.

Corncobs were collected in Cai Rang district, Can Tho city. They were then thoroughly washed several times in distilled water to remove water-soluble impurities and dried in an oven at 105°C for 24 hours before being preserved for final use.

2.2. Modified biochar preparation

Biochar was prepared by pyrolyzing corncob in a muffle furnace at three different temperatures, 400, 500, and 600°C, for 2 hours, with a heating rate of 10°C/minute. The biochar was milled and sieved to approximately 0.1 mm, washed with distilled water until the pH of the wash solution was nearly neutral, and dried in an oven at 105°C to obtain biochar materials, namely Bio 400, Bio 500, and Bio 600.

To prepare modified biochar, corncobs were immersed in an 8 M H_3PO_4 solution for 24 hours, then heated in a muffle furnace at 400, 500, and 600 °C with a 10 °C/min ramp for 2 hours. The solids obtained were washed with distilled water and then immersed in a 0.3 M NaOH solution for 24 hours. Then, they were washed several times, dried at 105ºC, and milled to produce modified biochar with a size of 0.1 mm, denoted as BioNaP 400, BioNaP 500, and BioNaP 600.

2.3. Biochar characterization

The BET (Joyner-Halenda) method was employed to determine the modified biochar's specific surface area and pore-size distribution. The pore structure analysis was carried out using nitrogen adsorption/desorption isotherms at a temperature of 77 K. Scanning electron microscopy (SEM, JCM-7000/JEOL, Japan) was utilized to investigate the surface morphology of the biochars. To examine the surface functional groups of the biochar, Fourier-transform infrared spectroscopy (FT-IR, PerkinElmer Frontier FT-IR/NIR) was applied, with measurements taken in the mid-infrared range of 400 to 4000 cm^{-1}. Thermogravimetric analysis (TGA) was used to monitor weight loss (TG signals) and the rate of weight loss (DTG signals) over the temperature range of 0 to 1000ºC. The concentration

of MV in the solution was measured using a UV-Vis spectrophotometer (Spectro UV-Vis Double Beam UVD-3500).

Batch adsorption investigations

MV crystals were dissolved in water to prepare antibiotic wastewater solutions at specific concentrations. Batch adsorption tests were performed to assess MV removal performance in terms of both adsorption efficiency and capacity. In each test, a finite amount of biochar was introduced into 20 mL of simulated wastewater and stirred at 400 rpm with a magnetic stirrer. After the reaction, the solution was separated by centrifugation for 10 min. The concentration of MV remaining in the solution was measured at 583 nm using a UV-Vis spectrophotometer to evaluate adsorption performance. All tests were conducted in triplicate to ensure reproducibility, and the average values were analyzed using statistical methods.

The removal efficiency (RE) and the adsorption capacity (Q_t) at time t were calculated according to Equations (1) and (2) as follows.

$$\text{RE}\ (\%) = \frac{C_0 - C_t}{C_0}.100 \quad (1)$$

$$Q_t\left(\frac{mg}{g}\right) = \frac{(C_0 - C_t).V}{w} \quad (2)$$

where C_0 (mg/L) and C_t (mg/L) are the initial and remaining MV concentrations at time t (mg/L), V(L) represents the solution volume, and w (g) is the mass of adsorbent.

2.4. Reusability investigation

The reusability and stability of the modified biochar were examined under the optimal MV removal conditions identified in previous sections. Then, in the adsorption process, the solid material was regenerated by first drying it and ultrasonically shaking it in a H_2O_2-methanol mixture (1:10 v/v) for 30 min. The solid was then collected by centrifugation, rinsed with distilled water, and dried again at 105 °C for 24 hours to restore the adsorbent. This process was repeated for five adsorption-desorption cycles.

2.5. Adsorption kinetics and isotherm models

A kinetic analysis explored the impact of reaction time on the adsorption capacity of modified biochar. Determining the adsorption mechanism is crucial for predicting the solid-liquid sorption interaction and the behavior of the process. The study applied four kinetic models to experimental data, including the pseudo-first-order (PFO, equation 3), pseudo-second-order (PSO, equation 4), and Intraparticle diffusion models (5) (Wang & Guo, 2020; Tovar et al., 2021; T. Wang et al., 2021).

$$Q = Q_e\left[1 - \exp\left(-\frac{k_1 t}{2.303}\right)\right] \quad (3)$$

$$\frac{t}{Q_t} = \frac{1}{k_2 Q_e^2} + \frac{t}{Q_e} \quad (4)$$

$$Q_t = k_i t^{0.5} + C \quad (5)$$

where Q_t (mg/g^{-1}) denotes the adsorption capacity at a time t; k_1 (1/min) and k_2 (1/g.min) are the rate constants for PFO and PSO; k_i refers to the intraparticle diffusion rate constant (mg/g.min$^{0.5}$). a is the initial sorption ratio (g/mg.min), and b refers to the desorption constant (g/mg), which is related to the extent of surface coverage and activation energy for chemisorption. For biochar, C reduces with enhanced surface heterogeneity and the number of hydrophilic groups.

Adsorption isotherms were performed to investigate the amount of MV adsorbed at equilibrium, providing insights into the potential adsorption capacity and behavior of biochar treatment. These isotherms can offer valuable physicochemical data to improve the sorption process. The experimental data were fitted to three isotherm models: Temkin (equation 6), Freundlich (equation 7), and Dubinin-Radushkevich (D-R model, equation 8), as follows (Tovar et al., 2021; Wang et al., 2021).

Temkin isotherm model.

$$Q_e = Bln(K_T.C_e) \quad (6)$$

Where B denotes the Temkin constant related to the adsorption heat, K_T is the equilibrium binding constant (mg/L).

Freundlich isotherm model.

$$q_e = K_F C_e^{1/n} \quad (7)$$

where K_F (mg/g.(L/mg)$^{1/n}$) and n represent the Freundlich rate constant referring to adsorption capacity and adsorption intensity, respectively.

Dubinin-Radushkevich isotherm model (D-R model).

$$q_e = q_0.\exp(-K_{DR}\varepsilon^2) \quad (8)$$

$$\varepsilon = RT\left(1 + \frac{1}{C_e}\right) \quad ; \quad E = \frac{1}{\sqrt{2K_{DR}}}$$

where K_{DR} (mol^2/kJ^2) is the D-R rate constant related to adsorption energy, E (kJ/mol^1) is the average adsorption energy per molecule of

adsorbate required to transfer one mole of the adsorbate from the solution to the adsorbent surface, ε denotes the Polanyi adsorption potential which is a function of temperature, R is the ideal gas constant, 8.314 J/(mol.K), and T is the absolute temperature (K).

The non-linear mathematical models were fitted and plotted in OriginPro 2022 v.9.9.0225 (SR1) software.

3. RESULTS AND DISCUSSION

3.1. Effect of heating temperature on MV removal

Preparation conditions are crucial to determining the properties of biochar, particularly its performance in removing contaminants from the liquid phase. Figure 1 shows the impact of treatment conditions on the MV removal performance of different biochar materials derived from corncob**Error! Reference source not found.**. Modified Biochar (BioPNa) demonstrated a significant enhancement in MV removal performance compared to pyrolyzed biochar, achieving a maximum value of 82.8% compared to 65.2% for unmodified biochar (Bio). This increase was due to chemical modification, which significantly improved the properties of biochar, including its specific surface area and porosity. However, the MV adsorption efficiency of BioPNa declined slightly, whereas with increasing treatment temperature, an increasing trend was observed for Bio. This could be attributed to the higher pyrolysis temperatures promoting the thermal degradation of organic compounds in the biomass feedstock, resulting in an enhancement of the surface area and porosity, which favors the overall adsorption capacity (Sajjadi et al., 2019). On the other hand, biochar activated by H_3PO_4 at lower temperatures retains a higher density of functional groups on the biochar surface, which facilitates interactions with water-soluble pollutants and polar organic compounds, even though its surface area may be limited (Sajjadi et al., 2018). Therefore, biochar modified at 400ºC (BioPNa 400) was selected for further characterization and experimental investigations of MV removal.

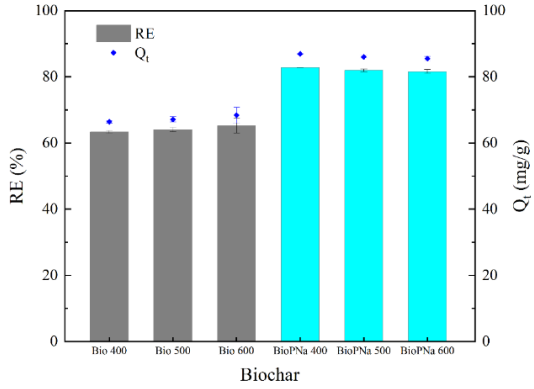

Figure 1. Effect of heating temperature of biochar on MV removal

3.2. Biochar characterization

The basic physicochemical properties of biochar treated at 400ºC are summarized in Table 1. It is noted that the modified biochar's specific surface area and pore volume have significantly increased to 989.14 m^2/g and 0.61 cm^3/g, which is substantially higher than those of Bio 400. It could be attributed to chemical activation with H_3PO_4 and NaOH at high temperatures, resulting in the formation of pores and an increased surface area (Sajjadi et al., 2019). Additionally, the surface morphology of biochar pyrolyzed at 400ºC and modified biochar is depicted in Figure 2. The surface of BioPNa 400 exhibited a rough, irregular, honeycomb-like structure and sharp-edged fragments, indicating that the biochar consists of a carbonaceous skeleton (Divband Hafshejani et al., 2016; Ghani et al., 2013). The porous structure of the biochar developed during the activation process resulted in a high specific surface area and large pore volume as tar, bound water, and organic substances were removed at elevated carbonization temperatures. Compared to Bio 400, BioPNa 400's surface had a richer porous structure. This may be attributed to H_3PO_4 and NaOH etching or removing parts of the biochar structure and its internal inorganic components, thereby increasing pore size and mesopore volume (Sajjadi et al., 2019).

Table 1. Basic physicochemical characteristics of biochar materials

Materials	C (wt.%)	O (wt.%)	P (wt.%)	S_{BET} (m^2/g)	Pore volume (cm^3/g)	Pore size (nm)
Bio 400	71.54	24.94	0.14	1.28	0.0037	0.78
BioPNa 400	77.87	20.63	0.47	989.14	0.61	2.71

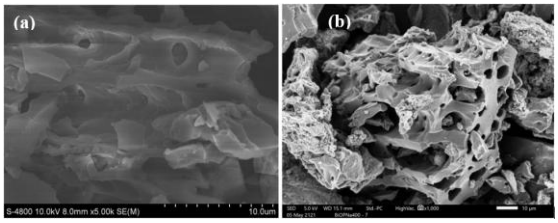

Figure 2. SEM image of Bio 400 (a) and BioPNa 400 (b)

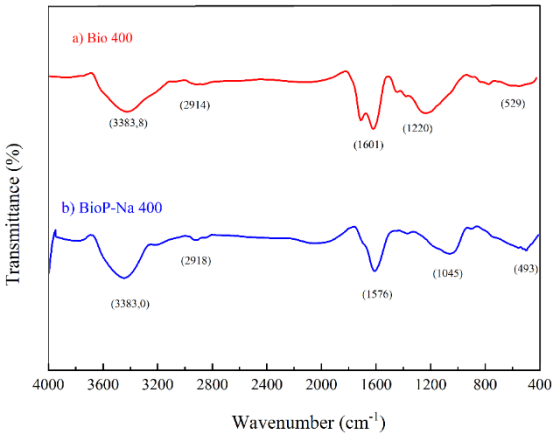

Figure 3. FT-IR spectra characterization of corncob-based biochar materials

Figure 3 presents FT-IR spectra of two biochar samples, which reveal the vibrational patterns of various functional groups on their surfaces, offering essential insights into their chemical makeup and potential reactivity. Both materials exhibit a broad peak around 3383 cm^{-1}, indicative of the stretching vibration band of the hydroxyl group (-OH), which may be linked to adsorbed water molecules, alcohol, or phenolic groups (Sajjadi et al., 2019). The C-H stretching vibration peaks appear at approximately 2914 cm^{-1}, and are typically associated with aliphatic hydrocarbons or aromatic compounds. Peaks at 1601 and 1576 cm^{-1} are attributed to C=C bond stretching in aromatic rings, a common feature of biochar due to its aromatic carbon structure. The C–O stretching vibration peak at 1220 cm^{-1}, likely related to C–O–C groups, alcohols, and ethers (Sajjadi et al., 2019), gradually vanished for BioPNa 400, while a new stretching vibration peak was found at 1045 cm^{-1} in the modified biochar, linked to the stretching of C-O bonds in ether groups or alcohols or possibly due to the formation of a P-O-P bond after phosphoric acid activation (Han, 2024). This is due to the crosslinking through the formation of phosphate and polyphosphate ester during the activation at high temperature (Sajjadi et al., 2019). The characterization results show that the chemical modification significantly enhanced the biochar's properties, including specific surface area, porosity, and functional groups on its surface.

3.3. MV removal experiments

3.3.1. Effect of pH solution

The pH level is a key factor influencing the interaction between the MV molecules and the porous material. The experiment aimed to determine the effectiveness of MV removal at pH levels from 6 to 12, which were selected because of the pHpzc (6.7) of BioPNa 400. As shown in Figure 4a, the MV removal efficiency remained relatively stable across this pH range, indicating that the pH solution did not significantly impact the MV removal capability of BioPNa 400. This could be attributed to the fact that the charge of MV, a cationic dye, can change with the pH level due to its structure. This dye typically contains amino groups ($-NH_2$) that can be protonated or deprotonated depending on the pH. In acidic conditions, methyl violet carries a more positive charge, whereas it becomes less positively charged or neutral at high pH levels. When the solution pH exceeds 6.7 (pHpzc), the BioPNa surface becomes negatively charged, reducing electrostatic attraction between MV and the adsorbent. This suggests that the effectiveness of MV adsorption on BioPNa was also affected by other adsorption mechanisms.

3.3.2. Effect of contact time

Figure 4b shows the impact of the contact time on MV removal performance. The removal effectiveness increased considerably by 11.2% and 11.7 mg/g for efficiency and adsorption capacity, respectively, within the first 10 minutes. As the contact time continued to increase, the performance remained mostly unchanged, at around 82% and 86 mg/g. Equilibrium was likely reached after 10 min of contact time. This trend may be due to the abundance of active sites on the surface of the porous material, leading to a rapid adsorption rate during the initial stage. As the contact time increased, the rate slowed significantly due to a decrease in unoccupied active sites and an increasing MV desorption rate, resulting in a slight increase in MV removal before equilibrium was reached.

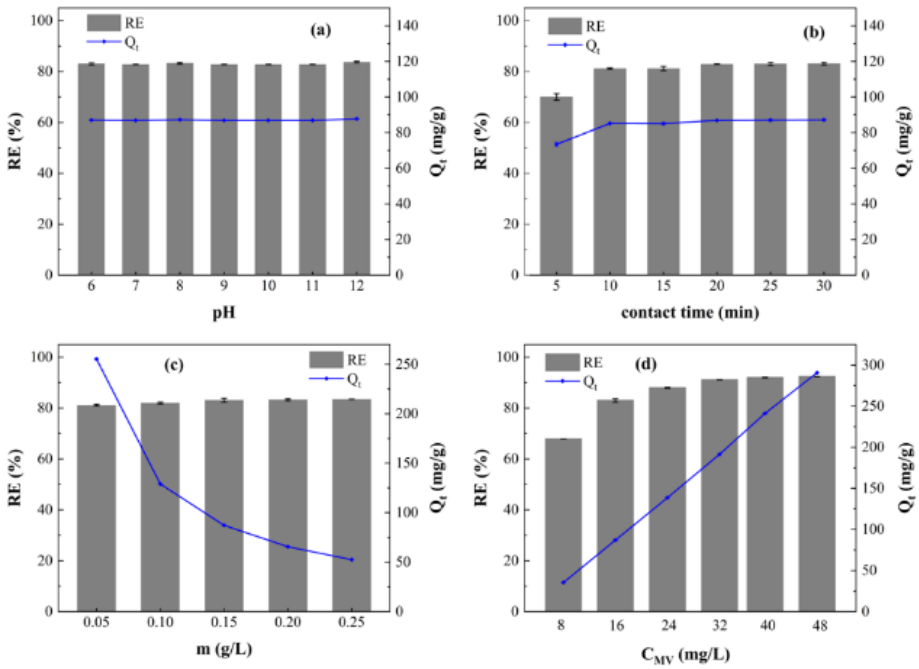

Figure 4. Effect of factors on MV removal performance: (a) pH solution, (b) reaction time, (c) mass dosage, and (d) MV concentrations

3.3.3. Effect of mass dosage of BioPNa

The mass dosage of porous material is crucial for MV removal from an aqueous solution. In this investigation, the influence of BioPNa mass dosage on MV removal effectiveness was evaluated over the range 0.05–0.25 g/L. As shown in Figure 4c, increasing the mass dosage slightly enhanced the removal efficiency by 2.4%, while the adsorption capacity decreased significantly by nearly 80% within this range. This increase in MV removal efficiency was attributed to the higher dosage, which provided more available adsorption sites on the biochar surfaces, thereby enhancing the interaction between BioPNa and MV. Furthermore, the removal rate reduced slightly as the dosage exceeded 0.15 g/L, consequently, further increases did not considerably increase the amount of MV adsorbed on the biochar's surface.

3.3.4. Effect of MV concentration

The initial MV concentration significantly affects removal efficiency, as the interaction between MV in an aqueous solution and the adsorbent is a crucial factor in determining how much MV is captured or bound to the surface of the porous material. In this experiment, the initial MV level varied from 8 to 48 mg/L. The removal efficiency increased from 68% to 92.4% within this concentration range. This behavior can be due to the higher amount of MV in the bulk solution, which results in more MV molecules being available to interact with the biochar surface. As the concentration continued to increase, adsorption sites on the porous material's surface became saturated. Consequently, the excess MV in the solution could not be absorbed, leading to no further change in removal efficiency.

3.3.5. Biochar reusability investigation

The regeneration and reusability of BioPNa were assessed over five cycles under the optimal conditions identified in the previous sections. After five cycles, the removal efficiency showed a minimal decline of just 4% (Figure 5a), demonstrating that BioPNa maintained its high effectiveness in removing MV during regeneration. The FT-IR spectra presented in Figure 5b reveal that most of the functional groups on BioPNa's surface persisted after five cycles, although their intensity had reduced compared to the original material. Additionally, minor damage was observed in the porous structure of the material at the fifth cycle Figure 5c. This suggests that the chemically activated biochar, sourced from agricultural waste, retains its high removal efficiency and structural stability after multiple cycles, indicating its potential for effective, industrial-scale wastewater treatment of MV with both high performance and good reusability.

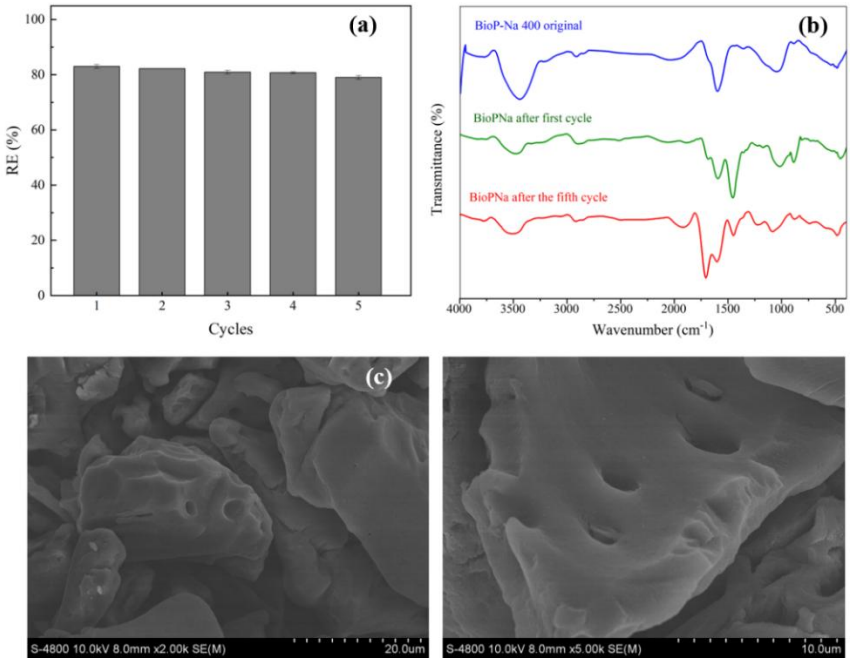

Figure 5. Recycling effectiveness of BioPNa for MV removal

3.3.6. Adsorption kinetics and isotherms

The study on adsorption kinetics focused on identifying the adsorption rate, the possible mechanisms, and factors influencing the adsorption process. Three kinetic models, including pseudo-first-order (PFO), pseudo-second-order (PSO), and intraparticle diffusion models, were applied to the measured data over a contact time range of 0 to 24 hours. Nonlinear estimation methods were applied because they provide more precise results than linearization (El-Khaiary et al., 2010; Ho, 2006). The results of the adsorption kinetics study are presented in Figure 6a and Table 2. PFO and PSO models were observed to be the best fit to the experimental data, each with a high R^2 (> 0.99). Additionally, the equilibrium adsorption capacity calculated from the PFO model ($Q_{e(cal)}$ = 86.77 mg/g) was in close agreement with the experimental data ($Q_{e(exp)}$ = 85.3 mg/g), suggesting that the adsorption of MV onto BioPNa is likely associated with a heterogeneous adsorption surface and physical adsorption behavior. This model assumes that adsorption mainly occurs in the initial stage with a few active sites at high initial MV concentration (Divband Hafshejani et al., 2016). Furthermore, these models with high R^2 (> 0.99) may indicate that the rate-limiting step of adsorption involves physicochemical interactions between the two phases, and that the adsorption rate depends on a mechanism at active sites on the BioPNa's surface (Tovar et al., 2021).

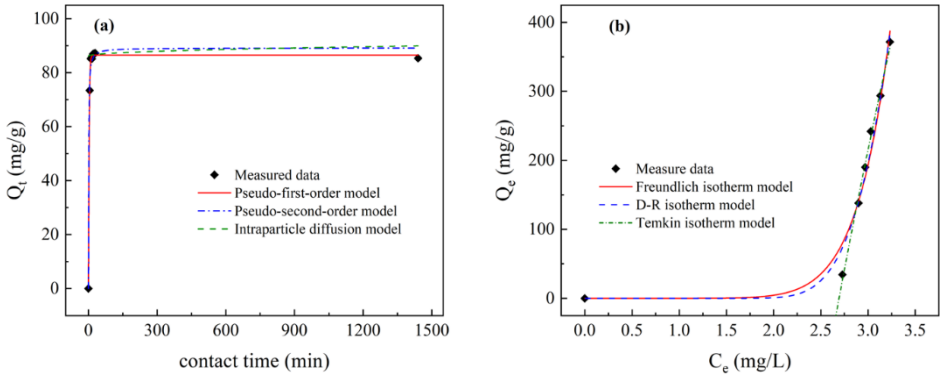

Figure 6. Adsorption kinetics (a) and adsorption isotherms (b) fitting curves for MV on BioPNa

Table 2. Kinetic parameters of MV adsorption by BioPNa

Pseudo-first order			Pseudo-second order			Intraparticle diffusion		
Q_e (mg/g)	k_1	R^2	Q_e (mg/g)	k_2	R^2	k_i	C	R^2
86.494	0.379	0.999	89.131	0.013	0.995	0.099	86.18	0.08

Table 3. Isotherm parameters of MV adsorption by BioPNa

Temkin			Freundlich model			D-R model	
A	B	R^2	K_F	n	R^2	E (kJ/mol)	R^2
0.3713	1993.1	0.997	0.0069	0.11	0.968	0.22	0.976

Adsorption isotherms were carried out to study the relationship between the concentration of MV in the bulk phase and its quantity absorbed by the BioPNa surface at equilibrium. These isotherms can provide valuable insights into the interaction between MV and the porous material during adsorption. Three isotherm models, including Temkin, Freundlich, and Dubinin-Radushkevich (D-R), were implemented to describe the adsorption behavior. The model estimations are presented in Figure 6b and Table 3.

The Temkin model showed the best fit to the measured data (R^2 = 0.997), indicating that the adsorption process involved chemisorption and is described by a uniform distribution of binding energies up to some maximum binding energy (Demiral, Şamdan, & Demiral, 2017; T. Wang et al., 2021). The Freundlich and the D-R models also exhibited high R^2 (> 0.96), with the Freundlich model yielding an n value of 0.11 (less than 1), corresponding to a poor adsorptive potential (Shikuku & Mishra, 2021). The average adsorption energy obtained from the D-R model was 0.22, suggesting the MV removal in this study was mainly governed by physisorption.

3.3.7. Possible adsorption *mechanisms*

According to the adsorption kinetics and isotherms, methyl violet adsorption likely follows physisorption due to the high specific surface area, large pore volume, and polarity of the modified biochar. Since MV's molecular diameter (approximately 1.24 nm (Muniandy, Salleh, & Zaini, 2020)) is smaller than the porous biochar's average pore size, MV molecules can fully penetrate the pores of the modified biochar. Furthermore, electrostatic attraction may contribute to adsorption due to the opposite charges on the surfaces of biochar and MV. The functional groups on the material surface, including hydroxyl and carboxyl groups, could interact efficiently with the amine groups in MV molecules through hydrogen bonds. Based on the structural characteristics of MV and the modified biochar, π-π interactions between the aromatic rings of MV and the conjugated π-electron systems in the biochar may also play a significant role in adsorption.

4. CONCLUSION

Modified biochar was successfully prepared from corncobs via chemical activation with NaOH and H_3PO_4 for methyl violet removal from aqueous solution. The batch adsorption investigations for methyl violet were performed by BioNaP. Characterization results indicated that chemical modification could significantly improve biochar properties, including high specific surface area, large pore volume, and abundant functional groups. The adsorption capacity could reach approximately 290 mg/g at high MV concentrations. The Pseudo-first-order and Temkin models can well describe the kinetic and isotherm adsorption process of BioPNa for MV, suggesting that the adsorption of methyl violet was dominated by physical adsorption. The adsorption mechanisms could include pore filling, electrostatic attractions, hydrogen bonds, and π-π interactions. The BioNaP also demonstrated high stability and reusability, maintaining its high removal effectiveness after five adsorption-desorption cycles. Therefore, the results provided a scientific basis for the comprehensive study of chemically modified biochar adsorbent for the treatment of methyl violet and organic dyes from wastewater.

ACKNOWLEDGMENT

The authors would like to thank Can Tho University for financial support (T2024-73), instrumental support, and valuable comments toward accomplishing this study.

CONFLICT OF INTEREST

The authors declare that they have no known competing financial interests or personal relationships that could have appeared to influence the work reported in this paper.

REFERENCES

Bustard, M., McMullan, G., & McHale, A. P. (1998). Biosorption of textile dyes by biomass derived from Kluyveromyces marxianus IMB3. *Bioprocess Engineering*, *19*(6), 427-430. https://doi.org/10.1007/PL00009028

Demiral, İ., Şamdan, C., & Demiral, H. (2017). Kinetics & equilibrium adsorption study of lead(II) onto activated carbon prepared from pumpkin seed shell. *Fresenius Environmental Bulletin*, *26*, 4484-4494. https://doi.org/10.1016/j.jcis.2004.06.042

Divband Hafshejani, L., Hooshmand, A., Naseri, A. A., Mohammadi, A. S., Abbasi, F., & Bhatnagar, A. (2016). Removal of nitrate from aqueous solution by modified sugarcane bagasse biochar. *Ecological Engineering*, *95*, 101-111. https://doi.org/10.1016/j.ecoleng.2016.06.035

El-Khaiary, M. I., Malash, G. F., & Ho, Y.-S. (2010). On the use of linearized pseudo-second-order kinetic equations for modeling adsorption systems. *Desalination*, *257*(1), 93-101. https://doi.org/10.1016/j.desal.2010.02.041

Fernandez, M. E., Nunell, G. V., Bonelli, P. R., & Cukierman, A. L. (2014). Activated carbon developed from orange peels: Batch and dynamic competitive adsorption of basic dyes. *Industrial Crops and Products*, *62*, 437-445. https://doi.org/10.1016/j.indcrop.2014.09.015

Ghani, W. A. W. A. K., Mohd, A., da Silva, G., Bachmann, R. T., Taufiq-Yap, Y. H., Rashid, U., & Al-Muhtaseb, A. A. H. (2013). Biochar production from waste rubber-wood-sawdust and its potential use in C sequestration: Chemical and physical characterization. *Industrial Crops and Products*, *44*, 18-24. https://doi.org/10.1016/j.indcrop.2012.10.017

Han, Y., Yin, Y. M., Zhang, H., Sun, S. J., Huang, Z. Z., Deng, Y. S. and Bao, L. (2024). Adsorption Effect of Phosphate Modified Grape Branch Biochar on Cd2. *Journal of Geoscience and Environment Protection*, *12*, 18. https://doi.org/10.4236/gep.2024.124005

Ho, Y.-S. (2006). Review of second-order models for adsorption systems. *Journal of Hazardous Materials*, *136*(3), 681-689. https://doi.org/10.1016/j.jhazmat.2005.12.043

Ho, Y. S. (2006). Isotherms for the Sorption of Lead onto Peat: Comparison of Linear and Non-Linear Methods. *Polish Journal of Environmental Studies*, *15*, 81-86.

Kumar, K. V., & Sivanesan, S. (2006). Pseudo second order kinetics and pseudo isotherms for malachite green onto activated carbon: Comparison of linear and non-linear regression methods. *Journal of Hazardous Materials*, *136*(3), 721-726. https://doi.org/10.1016/j.jhazmat.2006.01.003

Muniandy, S., Salleh, L., & Zaini, M. A. A. (2020). Evaluation of malachite green and methyl violet dyes removal by 3A molecular sieve adsorbents. *Desalination and Water Treatment*, *203*, 440-448. https://doi.org/10.5004/dwt.2020.26228

Nguyen, T.-B., Tran, D. P.-H., Nguyen, V.-T., Vo, T.-D.-H., Nguyen, H.-V., Tra, V.-T., Nguyen, T.-N.-A., Le, L.-T., Bui, X.-T. (2024). Utilization of Modified Biochar for Removal of Dyes From Industrial Effluent. In *Catalytic Applications of Biochar for Environmental Remediation: A Green Approach Towards Environment Restoration*, *1*, 23-44. https://doi.org/10.1021/bk-2024-1478.ch002

Pelekani, C., & Snoeyink, V. L. (2001). A kinetic and equilibrium study of competitive adsorption between atrazine and Congo red dye on activated carbon: the importance of pore size distribution. *Carbon*, *39*(1), 25-37. doi:https://doi.org/10.1016/S0008-6223(00)00078-6

Sajjadi, B., Chen, W.-Y., & Egiebor, N. O. (2019). A comprehensive review on physical activation of biochar for energy and environmental applications. *Reviews in Chemical Engineering*, *35*(6), 735-776. https://doi.org/10.1515/revce-2017-0113

Sajjadi, B., Zubatiuk, T., Leszczynska, D., Leszczynski, J., & Chen, W. Y. (2018). Chemical activation of biochar for energy and environmental applications: a comprehensive review. *Reviews in Chemical Engineering*, *35*(7), 777-815. https://doi.org/10.1515/revce-2018-0003

Shikuku, V. O., & Mishra, T. (2021). Adsorption isotherm modeling for methylene blue removal onto magnetic kaolinite clay: a comparison of two-parameter isotherms. *Applied Water Science*, *11*(6), 103. https://doi.org/10.1007/s13201-021-01440-2

Tovar, C., Villabona-Ortíz, Á., & González-Delgado, A. (2021). Removal of Nitrate Ions Using Thermally and Chemically Modified Bioadsorbents. *Applied Sciences*, *11*, 8455. https://doi.org/10.3390/app11188455

Tran-Nguyen, P. L., Ly, K.-P., Dang, H.-G., Nguyen, M.-N., Dang, V.-P., Tran, N.-P.-D., Santoso, S. P., Yuliana, M., Angkawijaya, A. E., Tran, T. B. Q., Tran, T. M. T., Khang, V. H. (2025). Effective removal of crystal violet in the aqueous solution using magnetic composites originated from sugarcane bagasse. *Chemical Papers*, *79*(4), 2207-2223. https://doi.org/10.1007/s11696-025-03918-8

Wang, J., & Guo, X. (2020). Adsorption kinetic models: Physical meanings, applications, and solving methods. *Journal of Hazardous Materials*, *390*, 122156. https://doi.org/10.1016/j.jhazmat.2020.122156

Wang, T., Zhang, D., Fang, K., Zhu, W., Peng, Q., & Xie, Z. (2021). Enhanced nitrate removal by physical

activation and Mg/Al layered double hydroxide modified biochar derived from wood waste: Adsorption characteristics and mechanisms. *Journal of Environmental Chemical Engineering*, *9*(4), 105184. https://doi.org/10.1016/j.jece.2021.105184

Yaashikaa, P. R., Kumar, P. S., Varjani, S., & Saravanan, A. (2020). A critical review on the biochar production techniques, characterization, stability and applications for circular bioeconomy. *Biotechnology Reports*, *28*, e00570. https://doi.org/10.1016/j.btre.2020.e00570

Yu, C., Qiu, J. S., Sun, Y. F., Li, X. H., Chen, G., & Zhao, Z. B. (2008). Adsorption removal of thiophene and dibenzothiophene from oils with activated carbon as adsorbent: effect of surface chemistry. *Journal of Porous Materials*, *15*(2), 151-157. https://doi.org/10.1007/s10934-007-9116-4

Zhang, Z., Zhang, M., Zhao, X., & Cao, J. (2024). High-efficient removal and adsorption mechanism of organic dyes in wastewater by KOH-activated biochar from phenol-formaldehyde resin modified wood. *Separation and Purification Technology*, *330*, 125542. https://doi.org/10.1016/j.seppur.2023.125542